Available online at www.sciencedirect.com

jmr&t Journal of Materials Research and Technology

www.jmrt.com.br

Original Article

Effect of sugar palm nanofibrillated cellulose concentrations on morphological, mechanical and physical properties of biodegradable films based on agro-waste sugar palm (*Arenga pinnata (Wurmb.) Merr*) starch

R.A. Ilyas[a,b,*], S.M. Sapuan[a,b,*], Rushdan Ibrahim[c], Hairul Abral[d], M.R. Ishak[e], E.S. Zainudin[b], M.S.N. Atikah[f], N. Mohd Nurazzi[a], A. Atiqah[g], M.N.M. Ansari[g], Edi Syafri[h], Mochamad Asrofi[i], Nasmi Herlina Sari[j], R. Jumaidin[k]

[a] Laboratory of Biocomposite Technology, Institute of Tropical Forestry and Forest Products, Universiti Putra Malaysia, 43400 UPM Serdang, Selangor, Malaysia

[b] Advanced Engineering Materials and Composites Research Centre, Department of Mechanical and Manufacturing Engineering, Universiti Putra Malaysia, 43400 UPM Serdang, Selangor, Malaysia

[c] Pulp and Paper Branch, Forest Research Institute Malaysia, 52109 Kepong, Selangor, Malaysia

[d] Department of Mechanical Engineering, Andalas University, 25163 Padang, Sumatera Barat, Indonesia

[e] Department of Aerospace Engineering, Universiti Putra Malaysia, 43400 UPM Serdang, Selangor, Malaysia

[f] Department of Chemical and Environmental Engineering, Universiti Putra Malaysia, 43400 UPM Serdang, Selangor, Malaysia

[g] Institute of Power Engineering, Universiti Tenaga Nasional, 43000 Kajang, Selangor, Malaysia

[h] Department of Agricultural Technology, Politeknik Pertanian, Payakumbuh, Indonesia

[i] Laboratory of Material Testing, Department of Mechanical Engineering, University of Jember, Kampus Tegalboto, Jember 68121, East Java, Indonesia

[j] Department of Mechanical Engineering, Mataram University, West Nusa Tenggara, Indonesia

[k] Fakulti Teknologi Kejuruteraan Mekanikal dan Pembuatan, Universiti Teknikal Malaysia Melaka, Hang Tuah Jaya, 76100 Durian Tunggal, Melaka, Malaysia

ARTICLE INFO

Article history:
Received 4 July 2019
Accepted 20 August 2019
Available online 30 August 2019

Keywords:
Sugar palm starch
Nanofibrillated Cellulose
Nanocomposites

ABSTRACT

Sugar palm (*Arenga pinnata*) fibres and starches are considered as agro-industrial residue in the agricultural industry. This paper aims to investigate the effect of different concentrations (0–1.0 wt%) of sugar palm nanofibrillated cellulose (SPNFCs) reinforced sugar palm starch (SPS) on morphological, mechanical and physical properties of the bionanocomposites film. The SPNFCs, having a diameter of 5.5 ± 0.99 nm and length of several micrometres, were prepared from sugar palm fibres via a high-pressure homogenisation process. FESEM investigation of casting solution displayed good miscibility between SPS and SPNFCs. The FTIR analysis revealed good compatibility between the SPS and SPNFCs, and there were existence of intermolecular hydrogen bonds between them. The SPS/sPNFCs with 1.0 wt%

* *Corresponding authors.*
E-mails: ahmadilyasrushdan@yahoo.com (R. Ilyas), sapuan@upm.edu.my (S. Sapuan).

https://doi.org/10.1016/j.jmrt.2019.08.028

Mechanical properties
High-pressure Homogenisation
Agro-waste

had undergone an increment in both the tensile strength and Young's modulus when compared with the SPS film, from 4.80 MPa to 10.68 MPa and 53.97 MPa to 121.26 MPa, respectively. The enhancement in water barrier resistance was led by reinforcing SPNFCs into the matrix, which resulted in bionanocomposites. The properties of bionanocomposites will be enhanced for short-life applications, such as recyclable container and plastic packaging through the incorporation of SPNFCs within the SPS bionanocomposites.

1. Introduction

Petroleum-based polymers for food packaging application are known for causing catastrophic impacts to the environment [1,2]. Scientists have been working on finding alternative sources for producing greener polymers to cater to this petroleum-based polymers limitation. There are few alternatives that could reduce the environmental impact; one of them is to substitute petroleum-based plastic with thermoplastic starch-based film. Apart from its incredible properties, such as effective reinforcement, it is also capable of being modified or blended with other polymers in order to 'engineer-up' their process, properties, economical base material, abundance, and is biodegradable in nature. [3–7]. However, according to Sahari et al. [8] and Sanyang et al. [9], due to the nature of the films, it has been described that starch-based films for food packaging application have low water resistance barrier and poor mechanical strength, which are delicate in structure, easy to dissolve, and complex in its fabrication process. These deficiencies have limited its applications, mainly for food packaging purposes [10,11]. Therefore, the improvement of mechanical and water barrier properties by utilising nanotechnology might be a good alternative on developing the films based on polymer nanocomposites through the use of nanotechnology comprising a nanometric filler.

The usage of nanocellulose as reinforcement in biocomposite fabrication for food packaging application has gained much interest the researchers worldwide in the past decades. The packaging films were proven to enhance their functional properties by using the method, as studied by Ilyas et al. [6]. These nanofibres have resulted in a great deal of concern due to their remarkable characteristic, for instance, high surface-area-to-volume ratio with abundant hydroxyl groups on their surface, excellent thermal, electrical and mechanical properties instead of other economical fibres [12–16]. Crop residue can be a useful source of cellulose nanofibre due to their annual renewability. In the past decades, there are many different agro-wastes that have been used in nanocellulose preparation, such as soy hull [17], sugarcane bagasse [18], wheat straw [19], pineapple leaves [20], rice straw [21], coconut husk fibres [22], water hyacinth fibre [23–28], and banana peels [29]. Sugar palm fibres and sugar palm stem (mainly composed of starch) are by-products of the processed sugar palm fruits and sap for food products in Malaysia. After these main products are extracted from the tree, the undesired components of the plant, such as sugar palm fibres and stem, are dumped, where they would decompose naturally. Since sugar palm fibres are rich in cellulose, the findings from a few studies have showed that sugar palm fibres have huge potential as reinforcing component in various high-performance polymer composite applications [30–34], hence, increasing its commercial value as by-product from sugar palm cultivation [35,36]. Thus, this present study continues with sugar palm-derived nanofibrillated cellulose reinforced with sugar palm starch biopolymer.

There are several methods of nanocellulose extraction from the sugar palm tree, which include chemical, mechanical or both thermo-mechanical approaches. However, in this study, high-pressure homogenisation (HPH) process was used to isolate chemically treated dilute slurries of cellulose fibres, in which these fibres were defibrillated at high pressure. HPH process can be categorized under mechanical approached. This high mechanical force promoted high fibrillation degree of cellulose fibres that resulted in the formation of homogeneous suspensions with more individualised fibres [37]. Thus, to investigate the potential of nanofibrillated cellulose as a reinforcing agent in polymer, the development and characterisation of sugar palm starch polymer composites were reinforced in the nanofibrillated cellulose.

To the best of our knowledge, no study on sugar palm nanofibrillated cellulose reinforced sugar palm starch biopolymer composites has been found in literature. Therefore, in order to maximise the utilisation of sugar palm residue, sugar palm stem was used to gain the starch used in this study, in which it served as matrix for the films; whereas the fibres were employed for the isolation of the nanofibrillated cellulose. The resulting bionanocomposites were characterised pertaining to their structural, morphological, crystallinity, physo-chemical, and mechanical properties.

2. Experimental

2.1. Materials and chemicals

In this work, the sugar palm starch (SPS) and sugar palm fibre (SPF) were extracted from the sugar palm tree located at Jempol, Negeri Sembilan, Malaysia. The chemical substances used in this experiment were sorbitol, glycerol, acetic acid (CH_3COOH), sodium chlorite ($NaClO_2$), and sodium hydroxide (NaOH), supplied by Sue Evergreen Sdn Bhd, Semenyih, Malaysia.

2.2. Sugar palm starch extraction and preparation

The sugar palm starch (SPS) was obtained from the stem of an amateur sugar palm tree. Initially, the tree was cut down

using a chainsaw and the mixture of woody fibre and starch powder from the interior part of the stem was collected. The mixture was washed prior to filtration to separate the starch and the fibre. The fibres remained on the top of the sieve, while water had carried the starch granules in the suspension and was collected in the container after passing through the sieve. Starch, which is denser than water, had settled at the bottom of the container and excess water flowed over the sides. After the process, the fibrous remnants, which was the by-product, were discarded and the wet starch was taken out from the container to be dried in open air for 30 min and finally dried out in an air circulation oven at 120 °C for 24 h.

2.3. *Sugar palm fibre extraction and preparation*

The SPF that was found to be naturally wrapped around the trunk of sugar palm trees from the bottom to the top was removed using an axe prior to grinding and screening in FRITSCH PULVERISETTE mill to a preferred size of 2 mm.

2.4. *Cellulose extraction*

Delignification and mercerisation techniques were used in the extraction of cellulose fibres from the SPF [38]. The preparation of holocellulose using a bleaching process that involved chlorination was carried out according to the ASTM D1104-56 [39]. Then, the ASTM D1103-60 [40] standard was employed on the holocellulose to produce α-cellulose.

2.5. *Isolation of sugar palm nanofibrillated cellulose (SPNFCs)*

2.5.1. *Mechanical pre-treatment*

A refining treatment before high-pressure homogenisation (HPH) process was required in order to enhance the fibres accessibility and processing efficiency. Hence, the sugar palm cellulose (SPC) was refined in 20,000 revolutions in a PFI-mill according to ISO 5264-2:2002 [41]. Improvement of both external and internal fibrillations had undergone the process of refining the fibres and the process had improved the flow of fibres and avoided clogging during fluidisation.

2.5.2. *Mechanical High-Pressurise Homogenisation (HPH)*

Nanofibrillated cellulose from sugar palm fibres cellulose was isolated by the process of high-pressure homogenisation (HPH). Typically, 1.8% of the fibre suspension was processed in a high-pressure homogeniser (GEA Niro Soavi, Panda NS1001 L, Parma, Italy). The samples were passed for 15 times through an intensifier pump that functioned to increase the pump pressure, followed by the interaction chamber that defibrillated the fibres by shear forces and impacts against the channel walls and colliding streams. During this process, fibres were broken down from being macro-sized to nano-sized to form slurries of nanofibrillated cellulose. The high-pressure homogeniser was maintained to operate at 500 bar and under a neutral pH. The temperature was not fixed at a certain value; however, the fluidisation process was temporarily stopped when the temperature of the suspension had gone up to approximately 90 °C, to prevent pump cavitation. The process was then continued when the samples had cooled down to approximately 45 °C. The NFCs suspensions were then collected and freeze-dried at −110 °C using ethylene gas as the medium and stored in a cool place prior to sample analysis [42].

2.5.3. *Preparation of the SPS/sPNFCs nanocomposite films*

Sugar palm starch/sugar palm nanofibrillated cellulose (SPS/sPNFCs) bionanocomposite films were prepared using the solution casting method. SPNFCs, starch, glycerol, sorbitol, and distilled water were mixed and sonicated together to obtain a homogenous nanocomposite film. SPNFCs solutions were prepared by mixing and sonicating them with 190 mL of distilled water with different concentrations of SPNFCs (0.1–1.0 wt% on the starch basis) for 30 min. Then, 10 g of SPS and plasticiser (30% on the starch basis) were mixed with the prepared solutions and stirred at 1000 rpm for 20 min at 85 °C in a disperser for the starch to gelatinise. This step was carried out to ensure that a uniform degradation of the starch granules and homogeneous dispersion was simultaneously formed. The ratio of plasticiser to the combination of sorbitol and glycerol used was 1:1. Next, the film-forming suspension was let to cool down under vacuum condition to get rid of air bubbles present in the suspension prior to casting of 45 g of the suspension into each petri dish of 15 cm in diameter. The dish and its content were put in an oven overnight at a set temperature of 40 °C. SPS films were also prepared without SPNFCs that served as the control experiment (designed as SPS film), while the nanocomposite films with different loading concentrations of 0.1, 0.2, 0.3, 0.4, 0.5, and 1.0 wt% SPNFCs were denoted as SPS/sPNFCs-0.1, SPS/sPNFCs-0.2, SPS/sPNFCs-0.3, SPS/sPNFCs-0.4, SPS/sPNFCs-0.5, and SPS/sPNFCs-1.0, respectively. Prior to performing any characterisation analysis, the ensuing films were stored for 7 days in the desiccator (23 ± 2 °C and 53 ± 1% RH) to guarantee the consistency of the water contained in the stored films.

2.6. *Characterisation*

2.6.1. *Field emission scanning electron microscopy (FESEM)*

The morphology of the films was examined using field emission scanning electron microscopy (FESEM). The FEI NOVA NanoSEM 230 machine (FEI, Brno-Černovice, Czech Republic) with a 3 kV accelerating voltage aided the realisation of the FESEM visualisation analysis. The entire samples were encapsulated in gold, using an argon plasma metalliser (sputter coater K575X) (Edwards Limited, Crawley, United Kingdom) to avoid charging.

2.6.2. *Transmission electron microscopy (TEM)*

The Philips Technai 20 TEM with a 200 kV accelerating voltage was utilised to display nanostructure images of the SPNFCs. Initially, the SPNFCs was let go through ultrasonication process for a period of 10 min. Afterwards, a drop of well-dispersed SPNFCs sample was dropped on a carbon-coated copper grid to be analysed by TEM microscopy.

2.6.3. *Film thickness of SPS/sPNFCs nanocomposite films*

The thickness of the films was determined using an advanced micrometre (Mitutoyo, Japan). Six replications of measure-

ments were carried out at random points for each film and an average value was calculated and recorded.

2.6.4. *Density of SPS/sPNFCs nanocomposite films*

Densimeter (Mettler-Toledo (M) Sdn. Bhd) was utilised in the density determination of the obtained nanocomposite films. Xylene was used to substitute distilled water as the immersing liquid to avoid uptake of water by the film samples. The samples were dried for 7 d in a desiccator that used P_2O_5 as the drying agent. The mass of nanocomposite film samples was measured (m) prior to immersing the nanocomposite films into the liquid of volume (V); hence, the density denoted as (ρ) was calculated from Eq. (1). Each test was carried out in 6 replicates.

$$\rho = \frac{m}{V} \quad (1)$$

2.6.5. *Fourier-transforms infrared spectroscopy (FTIR) analysis*

FTIR spectroscopy (Nicolet 6700 AEM, Thermo Nicolet Corporation, Madison WI, USA) was used in the detection of the possible changes in the functional groups in sugar palm fibre at different stages of extraction. 42 scans at a 4 cm^{-1} resolution ranging from 4000 to 500 cm^{-1} led to the recognition of the spectra of the samples with spatial dimensions of 10 mm × 10 mm × 3 mm. KBr-disk technique was utilised in the preparation of samples.

2.6.6. *X-ray Diffraction (XRD)*

The XRD patterns of the SPS and SPS/sPNFCs nanocomposite films were studied using Rigaku D/max 2500 X-ray powder diffractometer (Rigaku, Tokyo, Japan) fixed with CuKα radiation ($\lambda = 0.1541$ nm) in the 2θ range of 10–40°. Afterwards, the determination of the index of crystallinity of the samples X_c was made possible using the empirical technique reported by Segal et al. [43], as given in Eq. (2), where, I_{002} and I_{am} are the peak intensities of crystalline and amorphous materials, respectively.

$$X_c = \frac{I_{002} - I_{am}}{I_{002}} \times 100 \quad (2)$$

2.6.7. *Tensile properties*

All film samples were kept under the temperature of 23 ± 2 °C and 53 ± 1% RH in a climatically controlled room for 72 h. The samples tensile strength, Young's modulus and the elongation at the break determination were performed in accordance to ASTM D882-02 [44]. An Instron 3365 universal testing machine (High Wycombe, England) with a loading cell of 30 kg mass was employed in the analysis of the tensile properties of the bionanocomposite film samples. Initially, the samples were cut into strips of 10 mm × 70 mm. The strips were then clamped between two tensile holders, with the length of the gauge initially set to 30 mm. The pulling of the film strip was done at a crosshead speed of 2 mm/min. The recording of the parameter values, force (N) and deformation (mm) of the strips was carefully done, while the extension persisted. Ten different specimens were measured and the outcomes were averaged to give the mechanical properties.

2.6.8. *Statistical analysis*

The analysis of variance (ANOVA) on the obtained experimental results was performed in SPSS software. Tukey's test was employed to conduct a mean comparison at a 0.05 level of significance ($p \leq 0.05$).

3. Results and discussion

3.1. *Morphology of SPNFCs*

FESEM micrographs of sugar palm fibre (SPF), sugar palm bleached fibre (SPBF), sugar palm cellulose (SPC), and sugar palm refined fibre (Fig. 1) revealed their homogeneity and micrometric dimensions, whereas the TEM nanograph of sugar palm nanofibrillated cellulose (SPNFCs) showed their nanometric dimension. An image processing analysis program, Image J, using the FESEM and TEM images, are used to calculate the diameters of the fibres from all treatments. Gaussian line shape was used in the profile analysis with peak fitting program to describe the average diameter of fibres. The average diameters obtained for SPF, SPBF, SPC, SPPFI, and SPNFCs were approximately 212.01 ± 2.17 μm, 121.8 ± 10.57 μm, 11.87 ± 1.04 μm, 3.925 ± 0.26 μm, and 5.5 ± 0.99 nm, respectively, and the lengths of several micrometres are shown in Fig. 1(e). These clearly showed that the diameters of SPNFCs were almost 40 thousand times smaller than that of SPF. Moreover, the resultant image of Fig. 1(d) displayed the HPH treatment on sugar palm fibres and endorsed that the aqueous suspensions of SPNFCs isolated were determined to be stable though zeta potential analysis due to negatively charged (−34.2 mV), thus, making it unable to agglomerate. The yield obtained from the HPH isolation of SPNFCs was 92%. The resulting diameters for SPNFCs were in agreement with the average diameter of other agro-residue sources, such as banana (5 nm) [45], flax fibre (5 nm) [46] and potato tuber cell (5 nm) [47]. This reduction in the diameter of SPNFCs compared to SPF can be attributed to the removal of lignin, hemicellulose and disintegrated through the process of delignification, mercerisation, refining and high-pressure homogeniser on the raw SPF.

3.2. *Surface and cross-sectional morphology of the SPS/sPNFCs nanocomposite films*

FESEM was used in the examination of the microstructure and the interfacial adhesion of sugar palm starch and its reinforced bionanocomposites. Fig. 2 displays the FESEM micro-image of the surface morphology of SPS-based films with and without the addition of SPNFCs. Also, from Fig. 2, there is no trace of starch cracks or granular accumulation formed on the surface of SPS films. Control SPS films showed even surfaces and compacted structures. The image obtained via FESEM was similar to the work done by Dias et al. [48] for the control of rice flour films.

Moreover, the addition of SPNFCs (0.1 wt%) within a control SPS film (SPS/sPNFCs-0.1) revealed an even, random, smooth, and homogeneous distribution of SPNFCs inside the SPS matrix. However, as the high amount of SPFNCs nanofiller concentration was used (SPS/sPNFCs-1.0) (Fig. 2g), the frac-

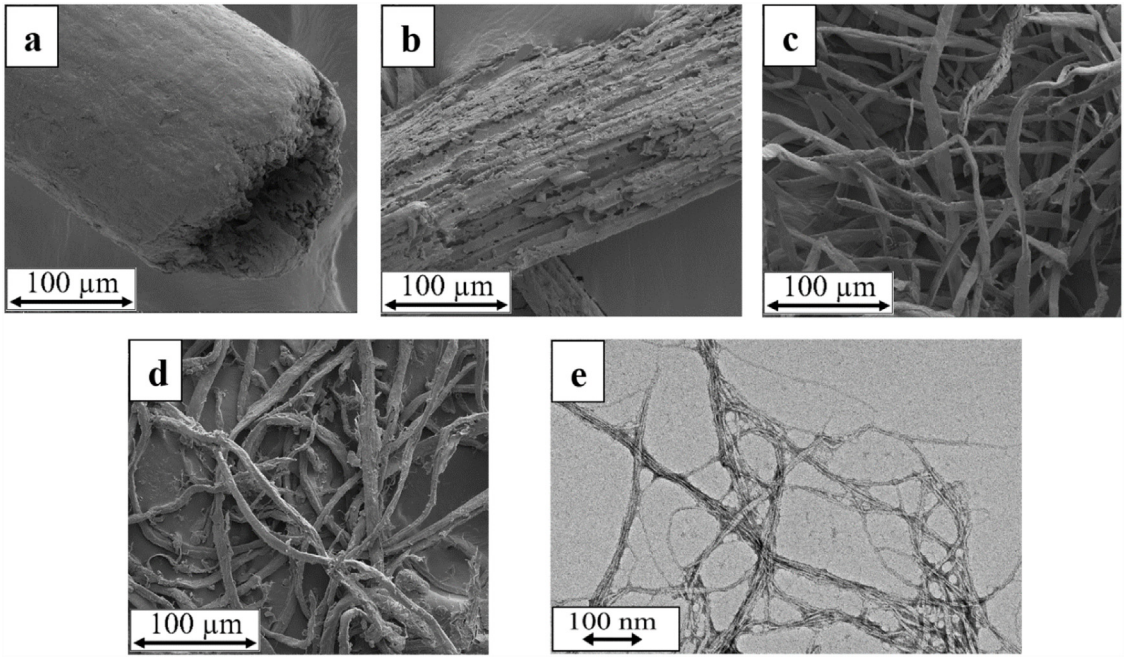

Fig. 1 – FESEM micrograph of: (a) raw sugar palm fibre; (b) sugar palm bleached fibre (SPBF); (c) sugar palm cellulose, (d) PFI refined fibre; and TEM nanograph of: (e) sugar palm nanofibrillated cellulose (SPNFCs).

tured surface area of SPS/sPNFCs-1.0 displayed relatively rough structures compared to controlled and low concentration SPNFCs films, indicating that the interfacial adhesion between SPNFCs and SPS starch polymer obtained was quite low. The cross-sections of the SPS/sPNFCs nanocomposites (0.1–0.5 wt%) (Fig. 2b–f) showed rougher structure than the SPS film as a result of the incorporation with SPNCCs as nanofiller. However, they seemed to be much smoother than the corresponding SPS/sPNFCs-1.0 nanocomposite film. Poor cracks and pores deformation within the thermoplastic starch indicated that a good distribution of nano reinforcements was attained. The addition of the SPNFCs nanofiller steered to the formation of more homogeneous surfaces, where nanofibres of the reinforcing material covered by the starch matrix were observed (Fig. 2b–g). The coating of the nanofibres with the starch matrix indicated that the nanofibre was physically reinforced in the network, which resulted from both nanofiller and matrix components that were highly compatible. Moreover, good adhesion between the nanofiller and the matrix had led to a resistant interface, subsequently reinforcing of the matrix enhanced the mechanical properties of the material. In addition, good adhesion between the matrix and the nanofibres can be justified, but there were no voids or pores present within the film. Besides that, there was no visible cluster or aggregation of SPNFCs observed (Fig. 2b–g). This was due to the nano-size of SPNFCs that made it almost invisible inside the matrix. Highly homogenous distribution and dispersion of SPNFCs in the SPS matrix were observed in low concentration of SPNFCs nanocomposites, which showed that the strong interactions among the SPNFCs themselves were partially destroyed, leading to a new strong interfacial adhesion between the SPNFCs nanofiller and SPS matrix film. Moreover, the "thread-like" SPNFCs were observable on the cross-section of the SPS/sPNFCs films, indicating an effective casting of the nanocomposite films. Other than that, the improvement in the compatibility between SPNFCs and SPS starch was attributed to the chemical structure similarities in cellulose and starch, nano-size effect from the SPNFCs, and hydrogen bonding interactions between nanofiller and matrix. This uniform distribution and strong nano-adhesion of the nano-filler in the matrix might play an important role in the improvement of the mechanical performance (i.e., high tensile strength) of the resulting nanocomposite films, as discussed in later section. Apart from that, these findings were validated by other studies, such as Besbes et al. [49] and Syafri et al. [16], in which the nanocomposite functional properties could be enhanced when the nanofibres are well distributed in the polymeric matrix. The lower opacity value of the films might be due to the roughness of the nanocomposites surface area. The addition of the nanocellulose into the starch matrix can be slightly observed in the nanocomposite, denoted by a translucent appearance, unlike the control SPS film that was transparent.

3.3. *Physical properties*

Table 1 shows similar thickness values with no significant difference observed for the control of SPS and SPS/sPNFCs nanocomposite films. This resulted from the strict control of the dry mass content per unit area of the plate during the solution casting procedure.

Besides that, a slightly significant difference was seen in the film density of control starch film and starch/sPNFCs nanocomposite films, as shown in Table 1. This was due to the low concentration of the nanofibre into the film matrix, where the SPNFCs was reported to have a low density of

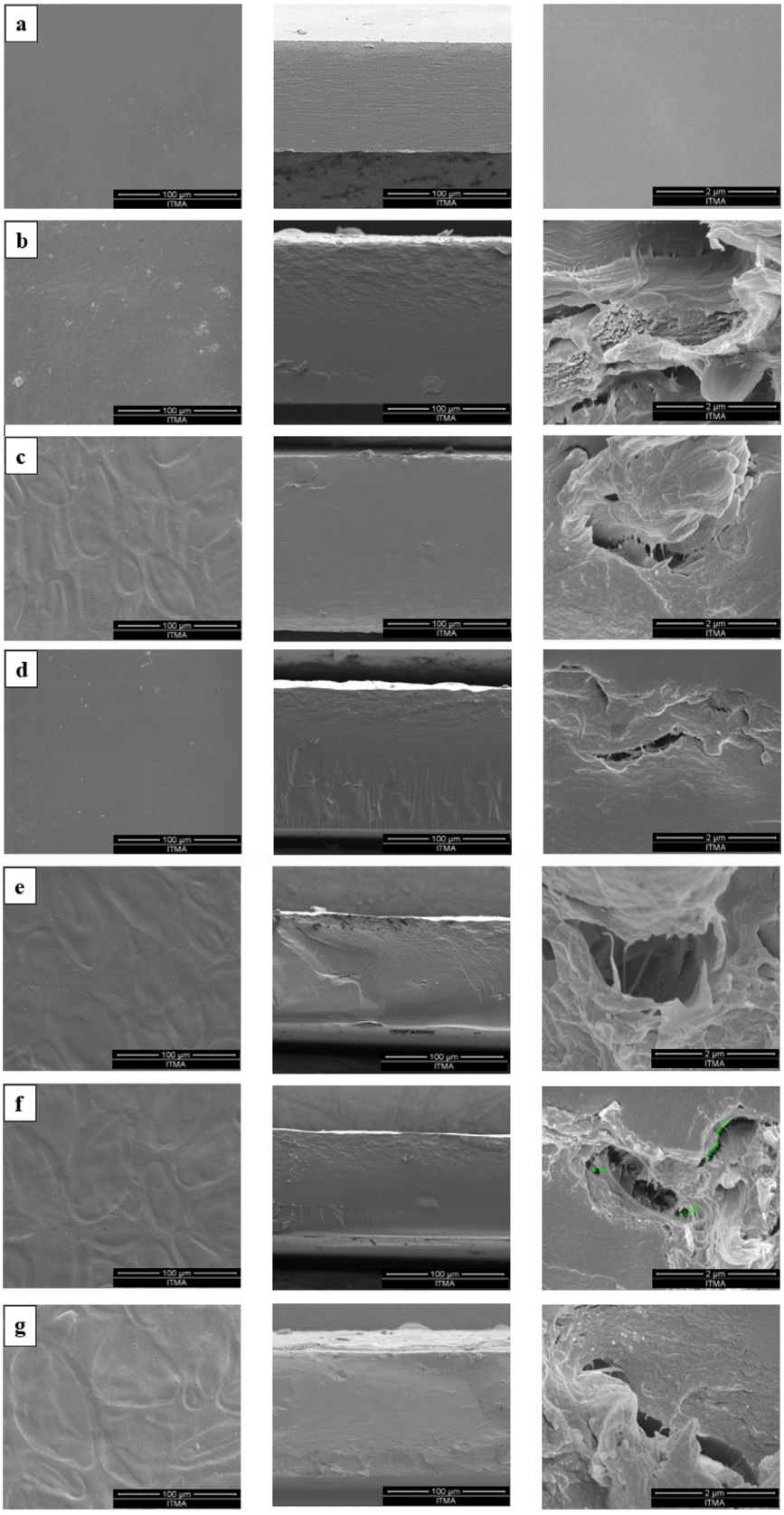

Fig. 2 – FESEM micrographs of the surface and cross-section of: (a) SPS, (b) SPS/sPNFCs-0.1, (c) SPS/sPNFCs-0.2, (d) SPS/sPNFCs-0.3, (e) SPS/sPNFCs-0.4, (f) SPS/sPNFCs-0.5, and (g) SPS/sPNFCs-1.0.

Table 1 – Physical properties of SPS and SPS/sPNFCs nanocomposite films with different concentrations of SPNFCs nanofillers.

	Thickness (μm)	Density (g.cm^{-3})	X_c (%)
SPS	123.6 ± 3.5^{a}	1.413 ± 0.01^{a}	22.81
SPS/sPNFCs 0.1	124.1 ± 2.8^{a}	1.423 ± 0.01^{b}	23.25
SPS/sPNFCs 0.2	123.2 ± 5.0^{a}	$1.430 \pm 0.00^{b,c}$	26.47
SPS/sPNFCs 0.3	123.6 ± 6.0^{a}	1.433 ± 0.01^{c}	33.59
SPS/sPNFCs 0.4	123.0 ± 6.5^{a}	1.433 ± 0.01^{c}	33.82
SPS/sPNFCs 0.5	124.1 ± 1.3^{a}	1.433 ± 0.01^{c}	40.35
SPS/sPNFCs 1.0	123.8 ± 4.5^{a}	$1.430 \pm 0.01^{b,c}$	43.363

Values with different letters in the same column are significantly different ($p < 0.05$).

1.1 ± 0.0026 g/cm^{-3}. In a recent cross-sectional study, Slavutsky & Bertuzzi [50] and Samir et al. [51] investigated that the densities of corn starch and poly(oxyethylene), respectively, are not affected by the reinforcement using nanocellulose as nanofiller. Nevertheless, the density of the nanofilms was increased upon nanofiller SPNFCs addition with an insignificant difference, as shown in Table 1. Higher density value was found for nanofilms with a higher concentration of NFC compared to the lower NFCs concentration. This might be associated with chemical properties of the nanofiller itself, whereby abundant hydroxyl groups are present in large surface area of SPNFCs (14.01 m^2/g) [52]. The strong interaction between the SPNFCs are partially destroyed during the sonication process, forming a new strong interfacial adhesion between the SPNFCs nanofiller and SPS matrix film. The formation of strong adhesion matrix/nanofiller had resulted in the reduction of free volume inside the SPS biopolymer, thus, making the structure more compact compared to the control starch.

3.4. *FTIR analysis of the SPS/sPNFCs Nanocomposites Films*

FTIR spectroscopy was used to identify the chemical structure of SPS and SPS/sPNFCs [53]. Fig. 3 presents the FTIR spectra of control SPS and SPS/sPNFCs nanocomposite films with different concentrations of SPNFCs. A sharp peak at 995 cm^{-1} was associated with the C—O bond from C—O—C groups. The band at 1335 cm^{-1} was related to the O—H of water. The small peak at 1644 cm^{-1} was assigned to C=O stretching, whereas the high peak displayed at 2925 cm^{-1} was corresponded to C—H stretching. Meanwhile, the broad peak of the SPS film observed at 3600 to 3020 cm^{-1} was assigned to the O—H group. These outcomes were also verified by Sanyang et al. [9] and Bourtoom and Chinnan [54] using sugar palm and rice starch film, respectively, where they observed the same peaks at 3600 to 3020 cm^{-1} referred to the O—H group. There were two phenomena that had occurred at the broad peak of 3600 to 3020 cm^{-1}, in which: (1) the relative peak strength of stretching vibrations for O—H groups in the FTIR spectra nanocomposite films weakened, and (2) band located at 3260 cm^{-1} were shifted to 3280 cm^{-1}, as the SPNFCs content changed from 0.1 to 1.0 wt%. It can be observed that the higher the concentration of the SPNFCs, the higher the shift. A possible explanation for these results might be due to: (1) an indication of the hydrogen bonding between the starch molecules that were partly destroyed, and (2) the new interactions by hydrogen bonding between the hydroxyl groups of sugar palm starch and SPNFCs. Moreover, the wavenumber of the peak for C—O stretching vibrations shifted from 995 to 992; this suggested that new interactions took place between nanofibrillated cellulose and starch molecules as a result of the addition of SPNFCs into the starch [55].

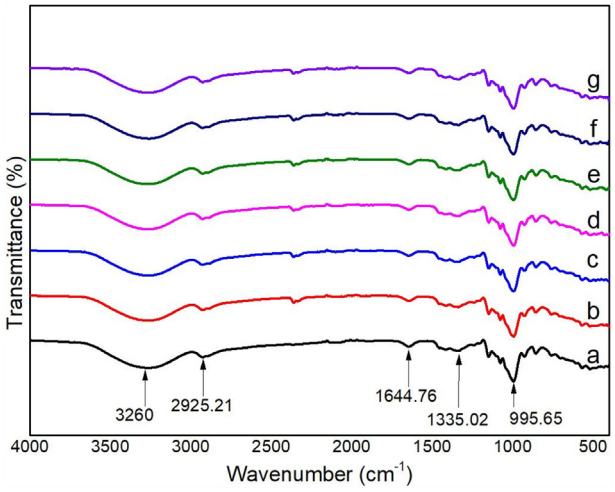

Fig. 3 – FTIR spectra of: (a) SPS, (b) SPS/sPNFCs-0.1, (c) SPS/sPNFCs-0.2, (d) SPS/sPNFCs-0.3, (e) SPS/sPNFCs-0.4, (f) SPS/sPNFCs-0.5, and (g) SPS/sPNFCs-1.0.

Apart from that, from Fig. 3, the SPS/sPNFCs nanocomposite films exhibited a similar IR spectrum compared with the control SPS film. The addition of SPNFCs showed a minor effect on the IR spectrum of SPS films due to lacking in new peaks formation. This result might be explained by the fact that both SPNFCs and SPS were composed of similar functional groups, which indicated a potential compatibility between the two components. Moreover, the correspondence between the IR spectra of control SPS film and SPS/sPNFCs nanocomposites film could be attributed to both SPS and SPNFCs originated from a single source; sugar palm tree. This circumstance explained that the inter- and/or intra-molecular interactions had existed between the starch and SPNFCs probably via the hydrogen bonding or the van der Waal's forces. These interactions increased with the increase of SPNFCs concentrations.

3.5. *XRD Analysis of the SPS/sPNFCs Nanocomposites Films*

To define the effect of concentration on the crystallinity of nanocomposite films, XRD analysis was performed and the corresponding diffractograms are shown in Fig. 4. Control SPS film exhibited a typical C-type crystallinity pattern, having peaks at $2\theta = 5.6^{o}$ that satisfied the characteristic of both A- and B-type polymorphs, as well as at 20.1 and 22.5^{o}; the characteristic of B-type polymorphs was perceived clearly [56]. Increasing the concentration of SPNFCs nanofibres was predicted to improve the relative crystallinity of the SPS based

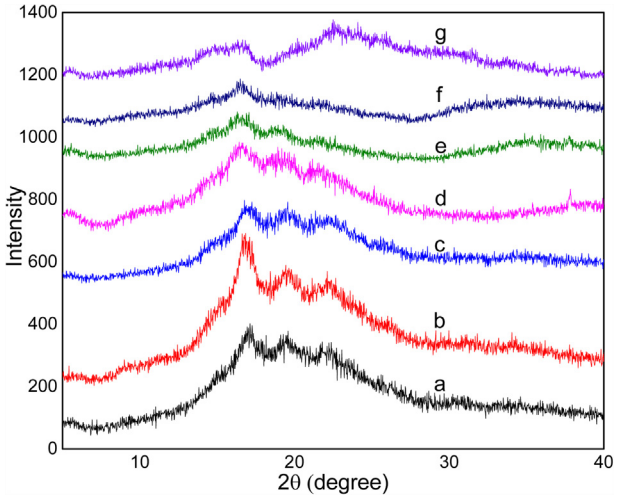

Fig. 4 – X-ray diffraction patterns of: (a) SPS, (b) SPS/sPNFCs-0.1, (c) SPS/sPNFCs-0.2, (d) SPS/sPNFCs-0.3, (e) SPS/sPNFCs-0.4, (f) SPS/sPNFCs-0.5, and (g) SPS/sPNFCs-1.0.

nanocomposites. Previous studies had discovered that crystallinity increment was attained by starch retrogradation, thus rose band narrowing that resulted in changes in absorbance ratios at certain peaks [56].

From Fig. 4, some diffraction peaks appeared in the diffractograms, as the concentration of SPNFCs increased in the starch. At SPNFCS content of 1.0 wt%, only one well-defined peak was observed at $2\theta = 22.6^{o}$ instead of two peaks ($2\theta = 15^{o}$), as a result of the addition of SPNFCs into the SPS matrix [57]. These diffraction peaks ($2\theta = 22.6^{o}$) can be observed in the 100 wt% of SPNFCs pattern at the same angle, which also indicated that these diffraction peaks in the nanocomposite materials were characterised by the SPNFCs nanofiller [37]. There were changes occurred in the diffraction peaks of SPS and SPS/sPNFCs nanocomposite films due to the variation in the concentrations of SPNFCs. The internal structure of the films had increased in crystallinity and become more orderly [58].

Moreover, when the SPNFCs were reinforced between the gaps existed between the starch molecules, the internal structure of bionanocomposite films became more orderly and the crystallinity of films was increased. It was observed that the increase in concentrations of SPNFCs nanofibres in the matrix resulted in the improvement of the relative crystallinity. SPNFCs extracted from the sugar palm fibres had high crystallinity (81.2%) and thus, their crystallinity was higher than the crystallinity of SPS film, leading to the improved crystallinity index of these nanocomposites.

The films crystallinity increased with the concentrations of the nanofiller. The relative crystallinity of the control SPS was 22.8%. This reinforcement led to an increase in the relative crystallinity from 22.81% to 43.36%. Table 1 presents the relative crystallinity of SPS and SPS/sPNFCs nanocomposite film data. Enhancement of the relative crystallinity of the SPS based composites was expected with the increasing amount of SPNFCs nanofiller.

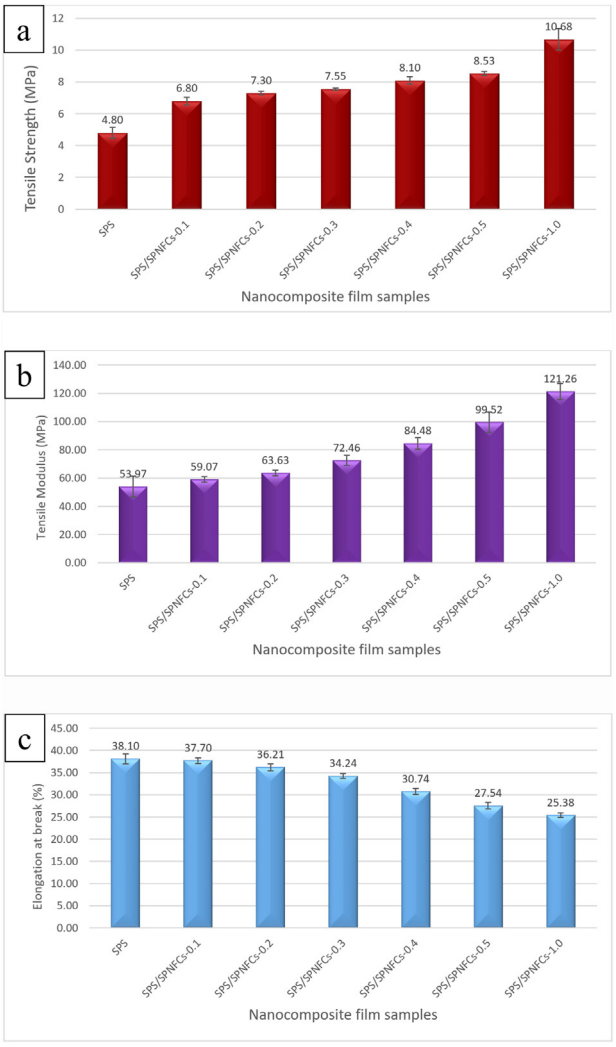

Fig. 5 – Effect of SPNFCs loading on the: (a) tensile strength, (b) tensile modulus, and (c) elongation at break (%) of SPS-SPNFCs nanocomposite films compared with control SPS films (For interpretation of the references to colour in this figure legend, the reader is referred to the web version of this article).

3.6. *Mechanical properties*

The mechanical properties of a material were strongly influenced by its microstructure that also provided essential information on the material interior structure. Fig. 5 and Table 2 show the mechanical properties of SPS/sPNFCs nanocomposites, which are the: (a) tensile strength, (b) tensile modulus, and (c) elongation at break. The results showed that the tensile strength and tensile modulus of SPS/sPNFCs nanocomposite films increased, as the SPNFC concentration increased from 0.1 wt% to 1.0 wt%. The tensile strength and tensile modulus of the control films were 4.8 MPa and 53.96 MPa, respectively. The addition of SPNFCs reinforcement from 0 to 1.0 wt% had considerably increased the tensile strength and modulus of the nanocomposite films from 6.80 to 10.68 MPa and 59.07 to 121.26 MPa, respectively. Therefore, at the maximum SPS loading (1.0 wt%), the tensile strength of SPS/sPNFCs-1.0 was

Table 2 – Tensile properties of SPS and SPS/sPNFCs nanocomposite films in different concentrations.

Samples	Tensile strength (MPa)	Tensile modulus (MPa)	Elongation at break (%)
SPS	4.80 ± 0.41^{a}	53.97 ± 8.74^{a}	38.10 ± 1.16^{f}
SPS/sPNFCs-0.1	6.80 ± 0.25^{b}	$59.07 \pm 2.10^{a,b}$	37.70 ± 0.66^{f}
SPS/sPNFCs-0.2	$7.30 \pm 0.11^{b,c}$	63.63 ± 2.09^{b}	36.21 ± 0.75^{e}
SPS/sPNFCs-0.3	$7.55 \pm 0.07^{c,d}$	72.46 ± 3.51^{c}	34.24 ± 0.55^{d}
SPS/sPNFCs-0.4	$8.10 \pm 0.23^{d,e}$	84.46 ± 4.21^{d}	30.74 ± 0.67^{c}
SPS/sPNFCs-0.5	$8.53 \pm 0.13^{e,f}$	99.52 ± 7.20^{e}	27.54 ± 0.76^{b}
SPS/sPNFCs-1.0	10.68 ± 0.67^{f}	121.26 ± 5.69^{f}	25.38 ± 0.50^{a}

Values with different letters in the same column are significantly different ($p < 0.05$).

improved by 122.50%, while the tensile modulus was 124.68% higher than that of the control SPS film. The increase in tensile and modulus and decrease in % ε were also observed; this can be ascribed to the favourable interaction between the SPNFCs and SPS polymer matrices, which facilitated adequate interfacial adhesion because of their chemical similarities [59]. Moreover, it was also indicated by the reinforcement effect from the homogeneously dispersed high-performance SPNFCs nanofiller in SPS matrix structure and the strong hydrogen bonding interaction between SPNFCs and SPS molecules during film-making process and drying of the nanocomposite, which restricted the chain motion of starch matrix.

Unlike the characteristics of tensile strength and tensile modulus, the elongation at break for the composite films decreased from 38.1 to 25.38%, as the SPNFCs concentration was increased from 0 to 1.0 wt%. This was due to the addition of SPNFCs concentration, which accidentally decreased the molecular mobility and ductility of the SPS matrix, making the composite materials stiffer. Thus, SPS/sPNFCs nanocomposite films had better resistant to break, less stretchable and stiffer than the control SPS films. The elongation at break decreased due to the rigid structure of the nanofiller, and this was supported with the previous result published in the literature [60].

There were similarities between the results expressed by Ramire & Dufresne [61], where the incorporation of nanocellulose within matrix polymer would improve the filler/matrix interactions generally lead to higher mechanical properties. From these studies, it was summarised that there were three main factors that had potentially affected the mechanical performances of the nanocomposite material: (1) the processing method, (2) the dimension and morphology of the nanofiller, and (3) the micro/nanostructure of the matrix and matrix/filler interface in this study. Nanofillers with a high aspect ratio of dimension were particularly remarkable due to their high specific surface area, resulting in improved reinforcing effects. According to Tonoli et al. [62], these nanofillers played an important role in the net adhesion formation within the matrix composite during the dewatering stage in the production process. Increasing the nanofibres aspect ratio and specific surface area with rough surface had subsequently reduced the fibre diameters and improved the nanofibre/matrix adhesion, while serving better mechanical features. The nanofibrillated cellulose from the sugar palm fibres showed similar effect to that of fibres from hemp [63] and ramie [64] on the mechanical properties in starch-based nanocomposites.

4. Conclusions

A suspension of sugar palm nanofibrillated cellulose (SPNFCs), with an average length of about several micrometres and diameters of 5.5 ± 0.99 nm were prepared from sugar palm fibres by high-pressure homogenisation method and was used to reinforce sugar palm starch matrix for the preparation of bionanocomposites via solution-casting method. The SPS/sPNFCs bionanocomposite films possessed higher mechanical properties (tensile strength and modulus) than control starch; nevertheless, it displayed lower elongation at break due to the addition of nano-reinforcements, which affected the segmental molecular chains mobility and ductility of starch biopolymer. FESEM micrographs displayed an adequate, good dispersion of SPNFCs within the SPS polymer and good adhesion between the polymer matrix and nanofibres. The addition of SPNFCs reinforcement from 0 to 1.0 wt% had considerably increased the tensile strength and modulus of the nanocomposite films from 6.80 to 10.68 MPa and 59.07 to 121.26 MPa, respectively. This was achieved due to the high compatibility between the two components, as a result of their chemical similarities. Therefore, this study has managed to explore a great potential of SPS/sPNFCs nanocomposite films for packaging applications.

Conflicts of interest

The authors declare no conflicts of interest.

Acknowledgments

The authors would like to thank Universiti Putra Malaysia for the financial support through the Graduate Research Fellowship (GRF) scholarship, Universiti Putra Malaysia Grant scheme Hi-CoE (6369107), Fundamental Research Grant Scheme FRGS/1/2017/TK05/UPM/01/1 (5540048) and iRMC UNITEN (RJO10436494).

REFERENCES

[1] Halimatul MJ, Sapuan SM, Jawaid M, Ishak MR, Ilyas RA. Effect of sago starch and plasticizer content on the properties of thermoplastic films: mechanical testing and cyclic soaking-drying. Polimery 2019;64:32–41, http://dx.doi.org/10.14314/polimery.2019.6.5.

[2] Halimatul MJ, Sapuan SM, Jawaid M, Ishak MR, Ilyas RA. Water absorption and water solubility properties of sago starch biopolymer composite films filled with sugar palm particles. Polimery 2019;64:27–35, http://dx.doi.org/10.14314/polimery.2019.9.4.
[3] Sanyang ML, Ilyas RA, Sapuan SM, Jumaidin R. Sugar palm starch-based composites for packaging applications. In: Bionanocomposites for packaging applications. Cham: Springer International Publishing; 2018. p. 125–47, http://dx.doi.org/10.1007/978-3-319-67319-6_7.
[4] Sapuan SM, Ilyas RA, Ishak MR, Leman Z, Huzaifah MRM, Ammar IM, et al. Development of sugar palm–based products: a community project. In: Sugar palm biofibers, biopolymers, and biocomposites. 1st ed. Boca Raton, FL: CRC Press/Taylor & Francis Group; 2018. p. 245–66, http://dx.doi.org/10.1201/9780429443923-12.
[5] Ilyas RA. Characterization of sugar palm nanocellulose and its potential for reinforcement with a starch-based composite. In: Sugar palm biofibers, biopolymers, and biocomposites. 1st ed Boca Raton, FL: CRC Press/Taylor & Francis Group; 2018. p. 189–220, http://dx.doi.org/10.1201/9780429443923-10.
[6] Ilyas RA, Sapuan SM, Ishak MR, Zainudin ES. Development and characterization of sugar palm nanocrystalline cellulose reinforced sugar palm starch bionanocomposites. Carbohydr Polym 2018;202:186–202, http://dx.doi.org/10.1016/j.carbpol.2018.09.002.
[7] Atikah MSN, Ilyas RA, Sapuan SM, Ishak MR, Zainudin ES, Ibrahim R, et al. Degradation and physical properties of sugar palm starch / sugar palm nanofibrillated cellulose bionanocomposite. Polimery 2019;64:27–36, http://dx.doi.org/10.14314/polimery.2019.10.5.
[8] Sahari J, Sapuan SM, Zainudin ES, Maleque MA. Mechanical and thermal properties of environmentally friendly composites derived from sugar palm tree. Mater Des 2013;49:285–9, http://dx.doi.org/10.1016/j.matdes.2013.01.048.
[9] Sanyang ML, Sapuan SM, Jawaid M, Ishak MR, Sahari J. Effect of sugar palm-derived cellulose reinforcement on the mechanical and water barrier properties of sugar palm starch biocomposite films. BioResources 2016;11:4134–45, http://dx.doi.org/10.15376/biores.11.2.4134-4145.
[10] Jumaidin R, Sapuan SM, Jawaid M, Ishak MR, Sahari J. Characteristics of thermoplastic sugar palm Starch/Agar blend: thermal, tensile, and physical properties. Int J Biol Macromol 2016;89:575–81, http://dx.doi.org/10.1016/j.ijbiomac.2016.05.028.
[11] Abral H, Basri A, Muhammad F, Fernando Y, Hafizulhaq F, Mahardika M, et al. A simple method for improving the properties of the sago starch films prepared by using ultrasonication treatment. Food Hydrocolloids 2019;93:276–83, http://dx.doi.org/10.1016/j.foodhyd.2019.02.012.
[12] Ilyas RA, Sapuan SM, Sanyang ML, Ishak MR, Zainudin ES. Nanocrystalline cellulose as reinforcement for polymeric matrix nanocomposites and its potential applications: a review. Curr Anal Chem 2018;14:203–25, http://dx.doi.org/10.2174/1573411013666171003155624.
[13] Kian LK, Jawaid M, Ariffin H, Karim Z. Isolation and characterization of nanocrystalline cellulose from roselle-derived microcrystalline cellulose. Int J Biol Macromol 2018;114:54–63, http://dx.doi.org/10.1016/j.ijbiomac.2018.03.065.
[14] Ilyas RA, Sapuan SM, Ishak MR, Zainudin ES. Sugar palm nanocrystalline cellulose reinforced sugar palm starch composite: degradation and water-barrier properties. IOP Conf Ser: Mater Sci Eng 2018;368, http://dx.doi.org/10.1088/1757-899X/368/1/012006.
[15] Syafri E, Kasim A, Abral H, Asben A. Cellulose nanofibers isolation and characterization from ramie using a chemical-ultrasonic treatment. J Nat Fibers 2018;00:1–11, http://dx.doi.org/10.1080/15440478.2018.1455073.
[16] Syafri E, Kasim A, Abral H, Sudirman, Sulungbudi GT, Sanjay MR, et al. Synthesis and characterization of cellulose nanofibers (CNF) ramie reinforced cassava starch hybrid composites. Int J Biol Macromol 2018;120:578–86, http://dx.doi.org/10.1016/j.ijbiomac.2018.08.134.
[17] Flauzino Neto WP, Silvério HA, Dantas NO, Pasquini D. Extraction and characterization of cellulose nanocrystals from agro-industrial residue – Soy hulls. Ind Crops Prod 2013;42:480–8, http://dx.doi.org/10.1016/j.indcrop.2012.06.041.
[18] de Morais Teixeira E, Bondancia TJ, Teodoro KBR, Corrêa AC, Marconcini JM, Mattoso LHC. Sugarcane bagasse whiskers: extraction and characterizations. Ind Crops Prod 2011;33:66, http://dx.doi.org/10.1016/j.indcrop.2010.08.009.
[19] Dufresne A, Cavaillé J-Y, Helbert W. Thermoplastic nanocomposites filled with wheat straw cellulose whiskers. Part II: effect of processing and modeling. Polym Compos 1997;18:198–210, http://dx.doi.org/10.1002/pc.10274.
[20] Cherian BM, Leão AL, de Souza SF, Thomas S, Pothan LA, Kottaisamy M. Isolation of nanocellulose from pineapple leaf fibres by steam explosion. Carbohydr Polym 2010;81:720–5, http://dx.doi.org/10.1016/j.carbpol.2010.03.046.
[21] Lu P, Hsieh Y. Preparation and characterization of cellulose nanocrystals from rice straw. Carbohydr Polym 2012;87:564–73, http://dx.doi.org/10.1016/j.carbpol.2011.08.022.
[22] Rosa MFM, Medeiros ES, Malmonge JAJ, Gregorski KS, Wood DF, Mattoso LHC, et al. Cellulose nanowhiskers from coconut husk fibers: effect of preparation conditions on their thermal and morphological behavior. Carbohydr Polym 2010;81:83–92, http://dx.doi.org/10.1016/j.carbpol.2010.01.059.
[23] Abral H, Dalimunthe MH, Hartono J, Efendi RP, Asrofi M, Sugiarti E, et al. Characterization of tapioca starch biopolymer composites reinforced with micro scale water hyacinth fibers. Starch/Staerke 2018;70:1–8, http://dx.doi.org/10.1002/star.201700287.
[24] Asrofi M, Abral H, Putra YK, Sapuan SM, Kim HJ. Effect of duration of sonication during gelatinization on properties of tapioca starch water hyacinth fiber biocomposite. Int J Biol Macromol 2018;108:167–76, http://dx.doi.org/10.1016/j.ijbiomac.2017.11.165.
[25] Asrofi M, Abral H, Kasim A, Pratoto A, Mahardika M, Hafizulhaq F. Mechanical properties of a water hyacinth nanofiber cellulose reinforced thermoplastic starch bionanocomposite: effect of ultrasonic vibration during processing. Fibers 2018;6:40, http://dx.doi.org/10.3390/fib6020040.
[26] Asrofi M, Abral H, Kasim A, Pratoto A, Mahardika M, Park JW, et al. Isolation of Nanocellulose from water hyacinth fiber (WHF) produced via digester-sonication and its characterization. Fibers Polym 2018;19:1618–25, http://dx.doi.org/10.1007/s12221-018-7953-1.
[27] Asrofi M, Abral H, Kasim A, Pratoto A, Mahardika M, Hafizulhaq F. Characterization of the sonicated yam bean starch bionanocomposites reinforced by nanocellulose water hyacinth fiber (WHF): the effect of various fiber loading. J Eng Sci Technol 2018;13:2700–15.
[28] Asrofi M, Abral H, Kasim A, Pratoto A. XRD and FTIR studies of nanocrystalline cellulose from water hyacinth (*Eichornia crassipes*) fiber. J Metastable Nanocryst Mater 2017;29:9–16, http://dx.doi.org/10.4028/www.scientific.net/JMNM.29.9.
[29] Pelissari FM, Andrade-Mahecha MM, Sobral PJ do A, Menegalli FC. Nanocomposites based on banana starch reinforced with cellulose nanofibers isolated from banana

peels. J Colloid Interface Sci 2017;505:154–67, http://dx.doi.org/10.1016/j.jcis.2017.05.106.
[30] Sahari J, Sapuan SM, Zainudin ES, Maleque MA. Effect of water absorption on mechanical properties of sugar palm fibre reinforced sugar palm starch (SPF/SPS) Biocomposites. J Biobased Mater Bioenergy 2013;7:90–4, http://dx.doi.org/10.1166/jbmb.2013.1267.
[31] Radzi AM, Sapuan SM, Jawaid M, Mansor MR. Mechanical performance of roselle/sugar palm fiber hybrid reinforced polyurethane composites. BioResources 2018;13:6238–49.
[32] Nurazzi NM, Khalina A, Sapuan SM, Ilyas RA. Mechanical properties of sugar palm yarn/woven glass fiber reinforced unsaturated polyester composites: effect of fiber loadings and alkaline treatment. Polimery 2019;64:12–22.
[33] Sapuan SM, Ilyas RA. Sugar palm: fibers, biopolymers and biocomposites. INTROPica 2017:5–7.
[34] Sapuan SM, Ishak MR, Leman Z, Ilyas RA, Huzaifah MRM. Development of products from sugar palm trees (*Arenga Pinnata Wurb. Merr*): a community project. INTROPica 2017:12–3.
[35] Mazani N, Sapuan SM, Sanyang ML, Atiqah A, Ilyas RA. Design and fabrication of a shoe shelf from kenaf fiber reinforced unsaturated polyester composites. In: Lignocellulose for Future Bioeconomy. Elsevier; 2019. p. 315–32, http://dx.doi.org/10.1016/B978-0-12-816354-2.00017-7.
[36] Ilyas RA, Sapuan SM, Ishak MR, Zainudin ES, Atikah MSN, Huzaifah MRM. Water barrier properties of biodegradable films reinforced with nanocellulose for food packaging application: a review. In: 6th Postgraduate Seminar on Natural Fiber Reinforced Polymer Composites 2018. Serdang, Selangor; 2018. p. 55–9.
[37] Ilyas RA, Sapuan SM, Ishak MR, Zainudin ES. Sugar palm nanofibrillated cellulose (*Arenga pinnata (Wurmb.) Merr*): effect of cycles on their yield, physic-chemical, morphological and thermal behavior. Int J Biol Macromol 2019;123:379–88, http://dx.doi.org/10.1016/j.ijbiomac.2018.11.124.
[38] Ilyas RA, Sapuan SM, Ishak MR, Zainudin ES. Effect of delignification on the physical, thermal, chemical, and structural properties of sugar palm fibre. BioResources 2017;12:8734–54, http://dx.doi.org/10.15376/biores.12.4.8734-8754.
[39] ASTM D1104-56. Method of test for holocellulose in wood. USA: American society for testing and materials; 1978.
[40] ASTM D1103-60. Method of test for alpha-cellulose in wood. USA: American society for testing and materials; 1977.
[41] ISO 5264-2. Pulps — Laboratory beating — Part 2: PFI mill method 2002.
[42] Ferrer A, Filpponen I, Rodríguez A, Laine J, Rojas OJ. Valorization of residual Empty Palm Fruit Bunch Fibers (EPFBF) by microfluidization: production of nanofibrillated cellulose and EPFBF nanopaper. Bioresour Technol 2012;125:249–55, http://dx.doi.org/10.1016/j.biortech.2012.08.108.
[43] Segal L, Creely JJ, Martin AE, Conrad CM. An empirical method for estimating the degree of crystallinity of native cellulose using the X-ray diffractometer. Text Res J 1959;29:786–94, http://dx.doi.org/10.1177/004051755902901003.
[44] ASTM D882-02. Standard test method for tensile properties of thin plastic sheeting; 2002.
[45] Zuluaga R, Putaux J-LL, Restrepo A, Mondragon I, Gañán P. Cellulose microfibrils from banana farming residues: isolation and characterization. Cellulose 2007;14:585–92, http://dx.doi.org/10.1007/s10570-007-9118-z.
[46] Bhatnagar A. Processing of cellulose nanofiber-reinforced composites. J Reinf Plast Compos 2005;24:1259–68, http://dx.doi.org/10.1177/0731684405049864.
[47] Alain D, Danièle D, Michel RV. Cellulose microfibrils from potato tuber cells: processing and characterization of starch-cellulose microfibril composites. J Appl Polym Sci 2000;76:2080–92, http://dx.doi.org/10.1002/(SICI)1097-4628(20000628)76:143.0.CO;2-U.
[48] Dias AB, Müller CMO, Larotonda FDS, Laurindo JB. Mechanical and barrier properties of composite films based on rice flour and cellulose fibers. LWT Food Sci Technol 2011;44:535–42, http://dx.doi.org/10.1016/j.lwt.2010.07.006.
[49] Besbes I, Rei M, Boufi S. Nanofibrillated cellulose from Alfa, Eucalyptus and Pine fibres: preparation, characteristics and reinforcing potential. Carbohydr Polym 2011;86:1198–206, http://dx.doi.org/10.1016/j.carbpol.2011.06.015.
[50] Slavutsky AM, Bertuzzi MA. Water barrier properties of starch films reinforced with cellulose nanocrystals obtained from sugarcane bagasse. Carbohydr Polym 2014;110:53–61, http://dx.doi.org/10.1016/j.carbpol.2014.03.049.
[51] Samir A, Alloin F, Sanchez J, El Kissi N, Dufresne A. Preparation of cellulose whiskers reinforced nanocomposites from an organic medium suspension. Macromolecules 2004;37:1386–93.
[52] Ilyas RA, Sapuan SM, Ibrahim R, Abral H, Ishak MR, Zainudin ES, et al. Sugar palm (*Arenga pinnata (Wurmb.) Merr*) cellulosic fibre hierarchy: a comprehensive approach from macro to nano scale. J Mater Res Technol 2019;8:2753–66, http://dx.doi.org/10.1016/j.jmrt.2019.04.011.
[53] Zhou C, Wu Q, Yue Y, Zhang Q. Application of rod-shaped cellulose nanocrystals in polyacrylamide hydrogels. Journal of colloid and interface science 2011;353:116–23, http://dx.doi.org/10.1016/j.jcis.2010.09.035.
[54] Bourtoom T, Chinnan MS. Preparation and properties of rice starch–chitosan blend biodegradable film. LWT Food Sci Technol 2008;41:1633–41, http://dx.doi.org/10.1016/j.lwt.2007.10.014.
[55] Cao X, Chen Y, Chang PR, Muir AD, Falk G. Starch-based nanocomposites reinforced with flax cellulose nanocrystals. Express Polym Lett 2008;2:502–10, http://dx.doi.org/10.3144/expresspolymlett.2008.60.
[56] Rindlava Å, Hulleman SHD, Gatenholma P. Formation of starch films with varying crystallinity. Carbohydr Polym 1997;34:25–30, http://dx.doi.org/10.1016/S0144-8617(97)00093-3.
[57] Frost K, Kaminski D, Kirwan G, Lascaris E, Shanks R. Crystallinity and structure of starch using wide angle X-ray scattering. Carbohydr Polym 2009;78:543–8, http://dx.doi.org/10.1016/j.carbpol.2009.05.018.
[58] Ilyas RA, Sapuan SM, Ishak MR. Isolation and characterization of nanocrystalline cellulose from sugar palm fibres (*Arenga Pinnata*). Carbohydr Polym 2018;181:1038–51, http://dx.doi.org/10.1016/j.carbpol.2017.11.045.
[59] Ilyas RA, Sapuan SM, Ishak MR, Zainudin ES. Water transport properties of bio-nanocomposites reinforced by sugar palm (*Arenga Pinnata*) nanofibrillated cellulose. J Adv Res Fluid Mech Therm Sci 2018;51:234–46.
[60] Savadekar NR, Mhaske ST. Synthesis of nano cellulose fibers and effect on thermoplastics starch based films. Carbohydr Polym 2012;89:146–51, http://dx.doi.org/10.1016/j.carbpol.2012.02.063.
[61] Ramires EC, Dufresne A. A review of cellulose nanocrystals and nanocomposites. Tappi J 2011;10:9–16.
[62] Tonoli GHD, Joaquim AP, Arsène M-A, Bilba K, Savastano H. Performance and durability of cement based composites

reinforced with refined sisal pulp. Mater Manuf Processes 2007;22:149–56, http://dx.doi.org/10.1080/10426910601062065.
[63] Cao X, Chen Y, Chang PR, Stumborg M, Huneault MA. Green composites reinforced with hemp nanocrystals in plasticized starch. J Appl Polym Sci 2008;109:3804–10, http://dx.doi.org/10.1002/app.28418.
[64] Lu Y, Weng L, Cao X. Morphological, thermal and mechanical properties of ramie crystallites—reinforced plasticized starch biocomposites. Carbohydr Polym 2006;63:198–204, http://dx.doi.org/10.1016/j.carbpol.2005.08.027.